Supporting Information for:

Degradation of sodium co-intercalation chemistry and ether-derived interphase on graphite anodes during calendar aging

Jiali Wang, [a] Junyang Hu, [a] Feiyu Kang *[a] and Dengyun Zhai *[a]

[a] Shenzhen Geim Graphene Center, Institute of Materials Research, Tsinghua Shenzhen International Graduate School, Tsinghua University, Shenzhen 518055, China

***Corresponding Author:**

Dengyun Zhai: zhaidy0404@sz.tsinghua.edu.cn;

Feiyu Kang: fykang@mail.tsinghua.edu.cn

Experimental Section.

1. Materials preparation. The $NaPF_6$ electrolyte was prepared with 1 M $NaPF_6$ (Guangdong Canrd New Energy Technology Co. Ltd) and diglyme (Sigma-Aldrich) in an argon-filled glovebox (O_2, H_2O <0.1 ppm).

Natural graphite materials were purchased from Shenzhen XFH Technology Co. Ltd. Graphite powders was dried in 80 ^oC oven.

The few-layer graphitic carbon (FGC) was prepared as described previously[1]: 8 g graphite and 4 g $NaNO_3$ (Aladdin) were added to 190 mL of 98 wt.% H_2SO_4 (Aladdin) at -5 ^oC. Next, 32 g $KMnO_4$ (Aladdin) was added slowly and held at -5 ^oC for 2h, then temperature was improved to 35 ^oC for 0.5 h under stirring and added 300 mL deionized water slowly. The reaction product was placed in 98 ^oC oil bath for 40 min, and 300 mL deionized water was added again. The resulting suspension was

vacuum filtered with 5 wt.% HCl and centrifugal washing with H_2O and dried at 80 ^oC for 48 h. The dried powder was pretreated at 1000 ^oC for 2 h at Ar flow with a heating rate of 5 ^oC min^{-1} and further heated to 2200 ^oC for 1 h at 3 ^oC min^{-1}.

2. Electrochemical methods. Electrodes were prepared via coating slurry on Cu foils. The slurry contains active materials and polyvinylidene fluoride (PVdF) binder at the weight ratio of 9:1 dispersed in N-methyl-2-pyrrolodone (NMP). The slurry was stirred for 5 h and dried in 100 ^oC vacuum oven overnight. Then the electrodes were punched into 1 cm^2 discs (12 mm in diameters) with the mass loading around 2.5 mg cm^{-2}. Electrochemical measurements used 2032-type coin-cells with 90 μL electrolyte. A glass fiber (Whatman, GF/A) and a Celgard 2320 were the separators of the cells. The Na counter electrodes were punched to 1 cm^2. The cells were assembled in argon-filled glove box.

The pre-cycled electrodes were carried out at 100 mA g^{-1} in voltage range of 0.01–2 V (vs. Na^+/Na) on a LAND-2001A battery tester. The static measurements for calendar aging were monitored voltage with a pause of various hours, when the electrodes were fully or partially discharge at 11st cycle. Graphite at SOC100 is discharged to 0.01 V, and the SOC60 is controlled discharge to 60% of reversible capacity (106 mAh g^{-1}).

Electrochemical impedance spectroscopy (EIS) was conducted in Na||graphite half-cell using Solartron 1470E workstation. And a frequency range of 100 kHz to 0.01 Hz was used with a perturbation amplitude of 10 mV. Distribution of relaxation time (DRT) was used to decouple Nyquist plots via DRTtools online algorithm, which is developed by Professor Francesco Ciucci's team[2, 3].

3. Materials characterization. The batteries were disassembled in argon-filled glovebox to prepare discharged or aged graphite electrodes. The phase transition of graphite during calendar aging were determined by X-ray diffraction (XRD) on Bruker D8 Advance diffractometer with Cu Kα (λ=0.154

nm). The electrodes for XRD were covered a Kapton tape to ensure airtightness during the testing process (within 10 min).

The cross-sectional morphology of graphite anodes at different states of charge (SOCs) were performed by scanning electron microscope (SEM) on HITACHI SU8010. Besides, a rolling process is used during electrode preparation to ensure the thickness consistency of graphite (Fig. S5). SEM samples were fixed on the SEM sample holders in a vacuum box and the box was transferred into SEM chamber through an antechamber to isolate air.

Atomic force microscope (AFM, Bruker Icon) experiments were conducted to characterize the mechanical properties of SEI in an Argon-filled glovebox. AFM nanoindentation was performed on the surface of samples using the PeakForce QNM mode. The AFM probe is RTESPA-300 from Bruker. The scan rate and maximum indentation force were set as 0.5 Hz and 250 nN, respectively. The imaging with a scan area of 300×300 nm^2 and 128×128 pixels provides high resolution to distinguish pristine graphite and cycled graphite. The Young's modulus was calculated by the Derjaguin-Müller-Toporov (DMT) model.

The HRTEM was characterized by FEI Tecnai G2 F30 microscope operated at 300 kV to describe the SEI evolution. The graphite electrodes were washed three times with 60 μL 1,2-dimethoxyethane (DME). Then a small amount of powder was scraps and dispersed in 300 μL DME. The sample was prepared by dropping 50 μL suspended liquid onto TEM grid. The prepared sample was placed in a vacuum box during the transfer process until the sample was inserted into the TEM column as quickly as possible for observation.

Graphite working electrodes were prepared in an argon-filled glovebox, rinsed with 60 μL DME for three times to remove residual Na salts and broken SEI. XPS signals were performed on a PHI 5000

VersaProbe II spectrometer using monochromatic Al Kα X-ray source with a vacuum transfer vessel. The obtained XPS data were calibrated with respect to the graphitic carbon peak at 284 eV in C1s spectrum.

For nuclear magnetic resonance (NMR), multiple graphite electrodes (16 mm in diameters) with a total mass of 45 mg were prepared to collect SEI. These working electrodes were washed with 60 μL DME for 6 times to remove the residual Na salts and broken SEI and placed in an argon-filled glovebox overnight to evaporate the solvent. Graphite electrodes were soaked in 700 μL 0.1 M DCl in D_2O solutions for 30 min. The 400 μL supernatant of extracted products was injected into a new and dried NMR tube. For pristine electrolyte, the 60 μL of electrolyte was injected, together with 340 μL 0.1 M DCl in D_2O solutions. Nuclear magnetic resonance (NMR) spectras were performed on a Bruker 400 MHz instrument at 25 °C, and the reference peak at 4.8 ppm was ascribed to HDO.

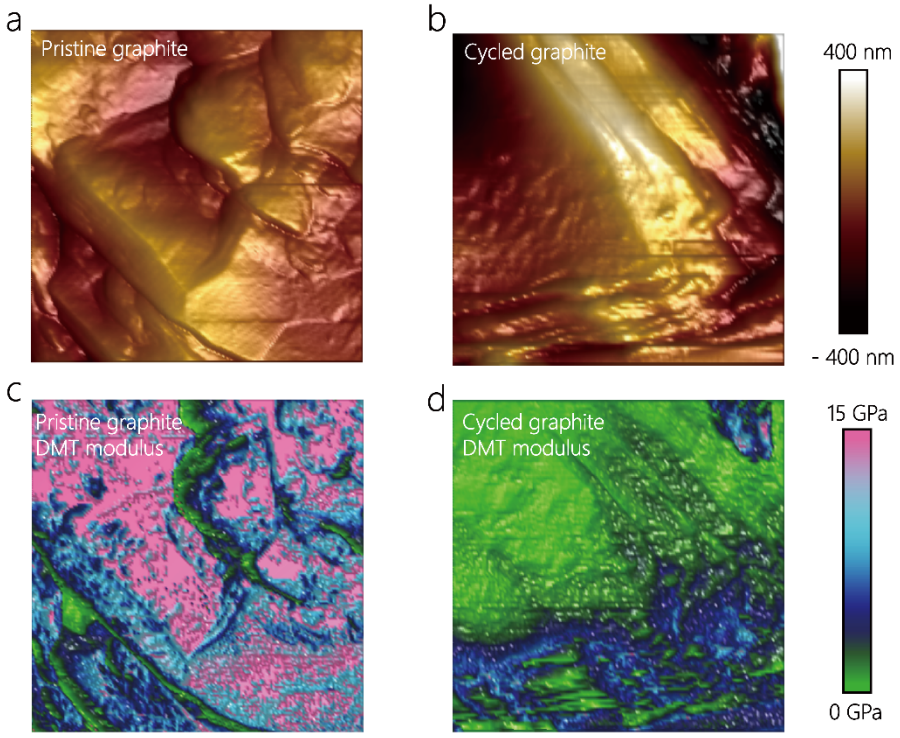

Fig. S1. (a–b) AFM images of pristine (a) and cycled (b) graphite. All scan sizes are 300×300 nm^2. The layered edges of bulks were confirmed to be characteristic of graphite. Compared with pristine graphite, the morphology of cycled graphite shows increased fluctuations. (c-d) DMT modulus of pristine (c) and cycled graphite (d). The average DMT modulus of pristine graphite is 12366 Mpa and diglyme-derived SEI exhibits the average DMT modulus of 1026 Mpa.

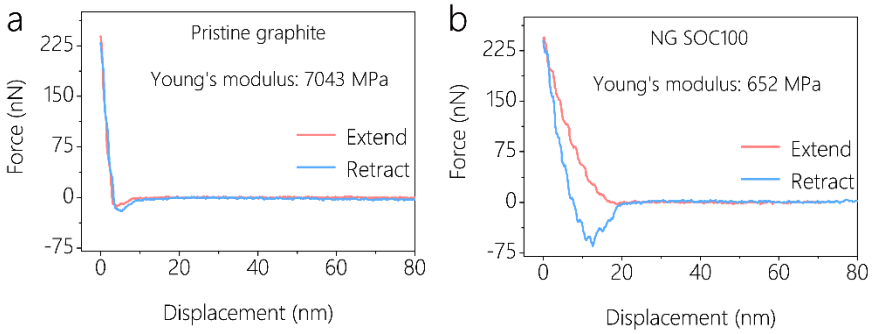

Fig. S2. Representive force-displacement curves of pristine graphite (a) and NG at SOC100 (b). During approaching process, the diglyme-derived SEI undergoes elastic deformation, thus Young's modulus were calculated by DMT model using the extend curves. Additionally, SEI exhibited no failure under a force of 250 nN, thus SEI thickness cannot determinate through AFM.

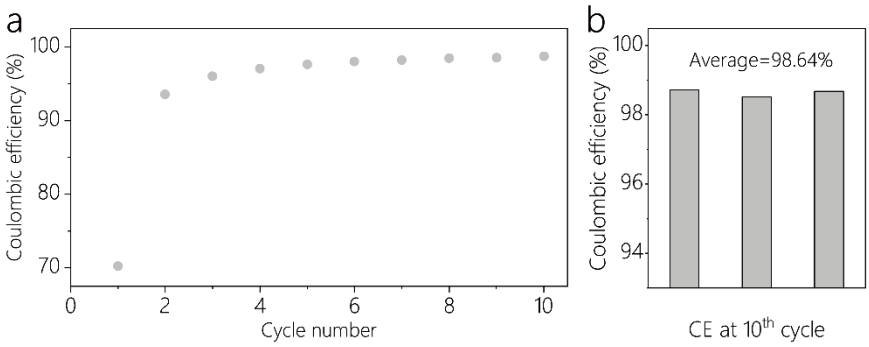

Fig. S3. Coulombic efficiency (CE) of graphite carbon during pre-cycling. (a) CE of graphite during cycle at 100 mA g^{-1}. (b) Three representative CE values of graphite at 10^{th} cycle, which is over 95% after 10 cycles.

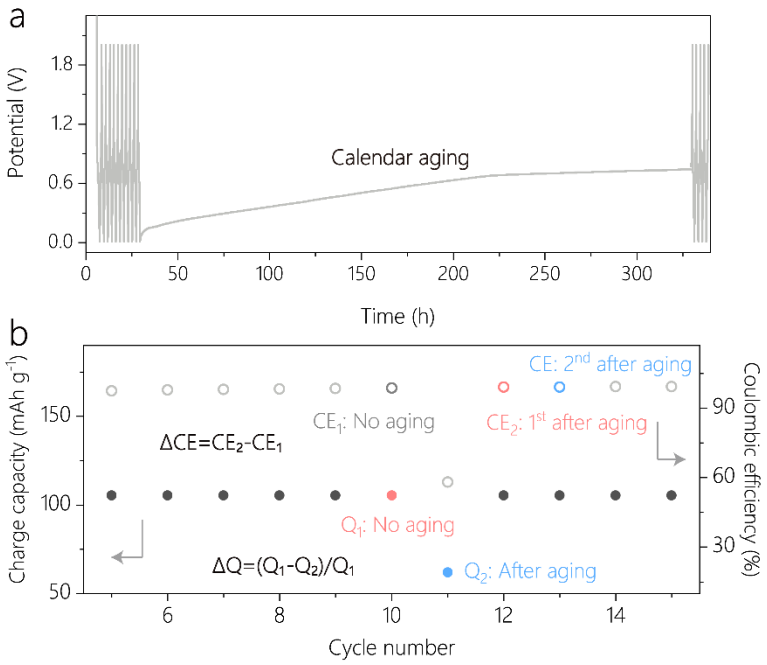

Fig. S4. Detailed parameters for capacity loss and CE. (a) Potential curves of graphite at SOC100 during calendar aging. (b) Charge capacity and CE of graphite anodes during calendar aging to describe the indictors to evaluate capacity loss and CE. CE_1 is CE of graphite anode before aging, and CE_2 is first cycle CE of graphite anode after aging. Q_1 is the charge capacity before aging, and Q_2 is the residual charge capacity after aging.

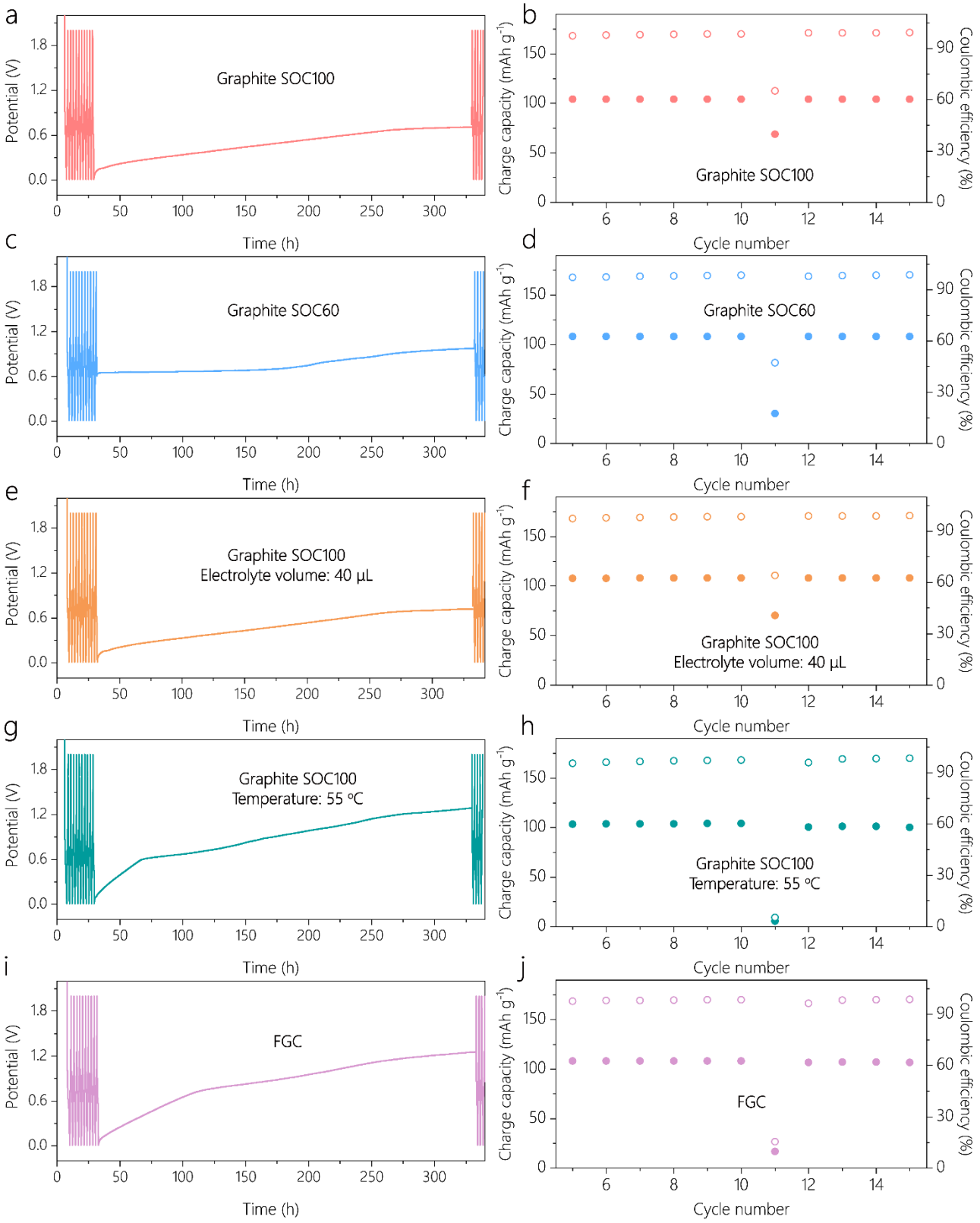

Fig. S5. The potential curves, charge capacity and CE in diglyme systems during 300 h calendar aging, including SOC states, less electrolyte volume (40 µL), high operation temperature (55 °C) and large specific surface area of carbon materials (FGC).

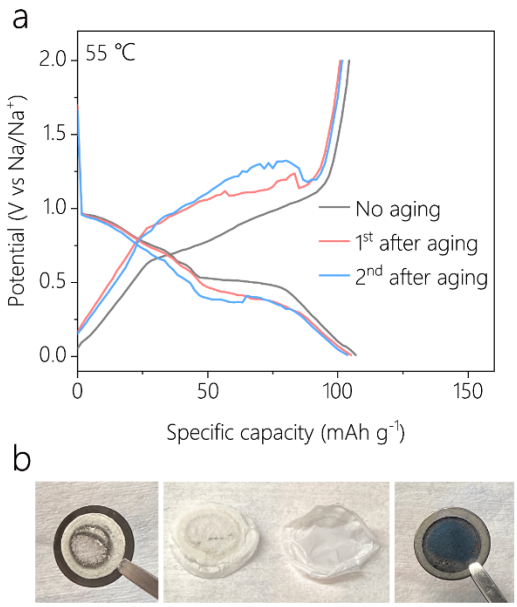

Fig. S6. Effect of high temperature on battery performance during calendar aging. (a) GCD curves of graphite before and after aging at 100 mA g^{-1}. (b) Photographs of Na, separators and discharged graphite after aging. After aging, the potential curves of graphite anode are abnormal, which may be contributed to the severe electrolyte decomposition.

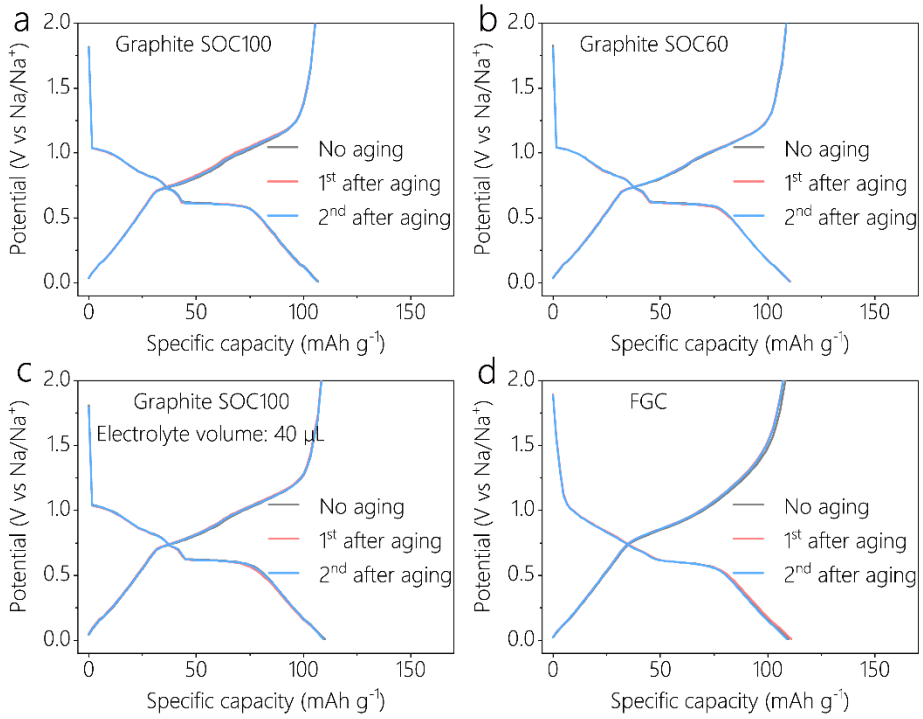

Fig. S7. (a–d) GCD curves of graphite before and after aging at 100 mA g^{-1}, including graphite at SOC100 (a), graphite at SOC60 (b), less electrolyte volume (c) and large specific surface area of carbon materials (d).

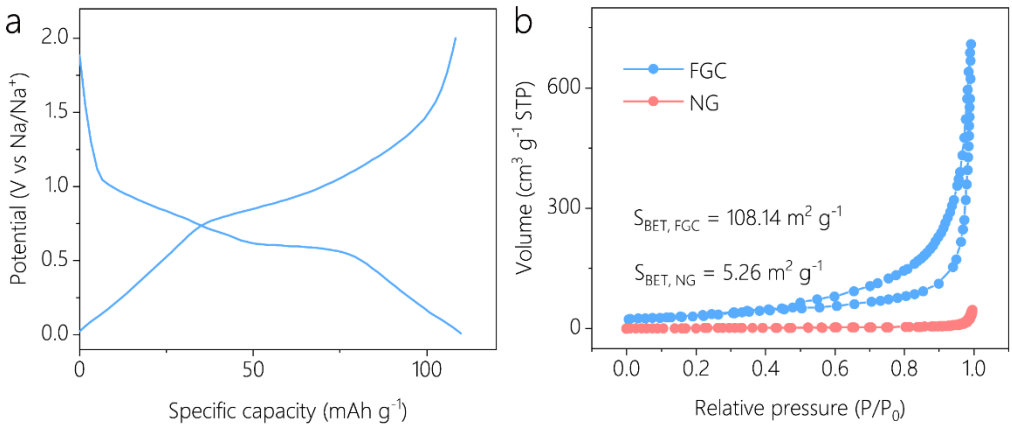

Fig. S8. Electrochemical curves and characterization of FGC. (a) GCD curve of FGC at 100 mA g^{-1}. (b) Nitrogen adsorption-desorption isotherm comparison of graphite and FGC. Although FGC is still co-intercalation behavior, its specific surface area is much higher than NG.

Table S1. The peak positions of different t-GICs in XRD patterns. The peaks were indexed as (00l) by applying Bragg's law[4].

Sample	2θ/°		
Graphite	(002) 26.67		
Stage 1 GIC	(002) 15.13	(003) 22.80	(004) 30.58
Stage 2 GIC	(004) 23.64	(005) 29.82	
High stage GIC	25.58	27.58	

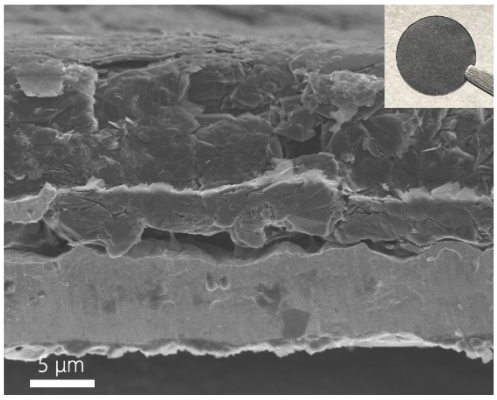

Fig. S9. Cross-section SEM image of pristine graphite. The inset is the photograph of graphite. The thickness of pristine graphite electrode is 15 µm, which is much thinner than the aged SOC60. This observation was also reported by in-situ electrochemical dilatometry previously[5].

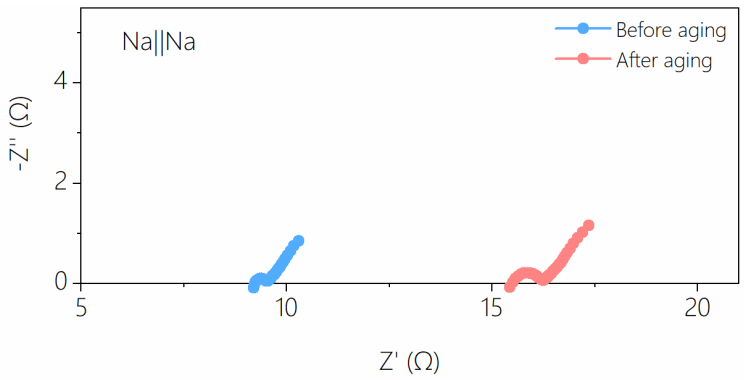

Fig. S10. Nyquist plots of Na||Na symmetrical cell before and after aging. The slight increase of resistance in aged Na||Na cell is not the same order of magnitude as graphite, thus the impact of Na counter electrode on resistance can be ignored in the half-cell analysis. The use of excess metallic Na in the half-cell further reduces its effect.

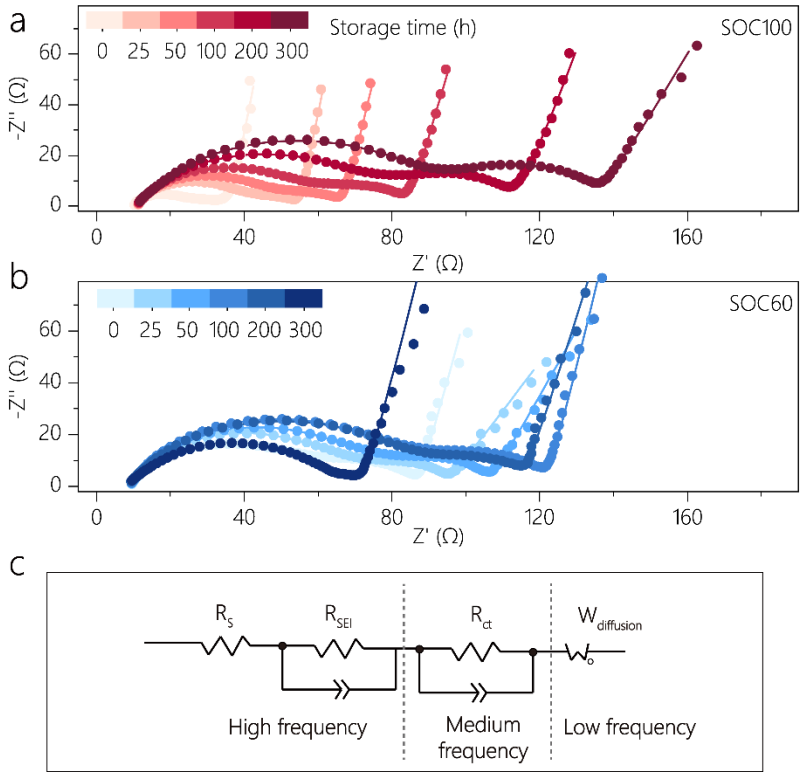

Fig. S11. (a–b) The Nyquist plots of graphite at SOC100 (a) and SOC60 (b) during 300 h calendar aging. (c) The equivalent circuit for impedance fitting of Nyquist plots.

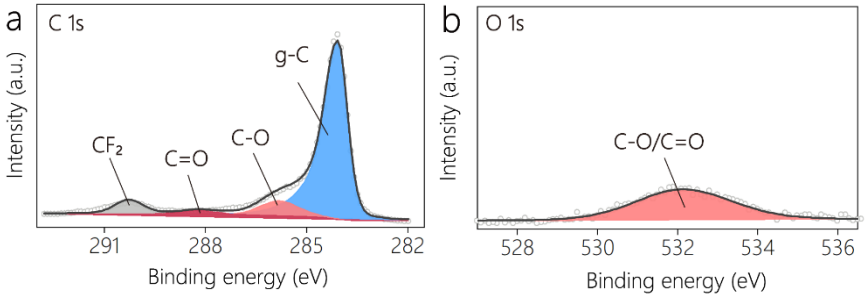

Fig. S12. XPS spectra of C 1s (a) and O1s (b) of graphite. The oxygen in graphite is limited, and the CF_2 at 290.4 eV is corresponds to PVDF in graphite electrode. The position of graphitic carbon in C 1s is 284 eV.

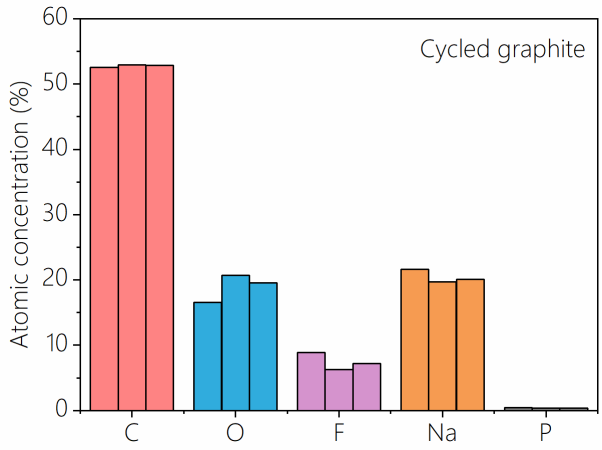

Fig. S13. The atomic composition radios of cycled graphite from XPS surface characterization. The content values are calculated from the fitting results of three different samples.

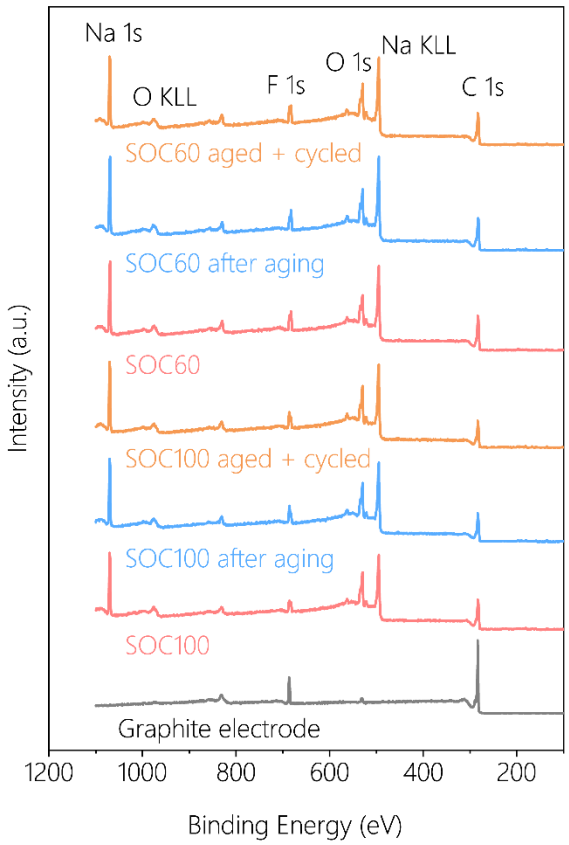

Fig. S14. XPS full spectra of graphite anodes at different states.

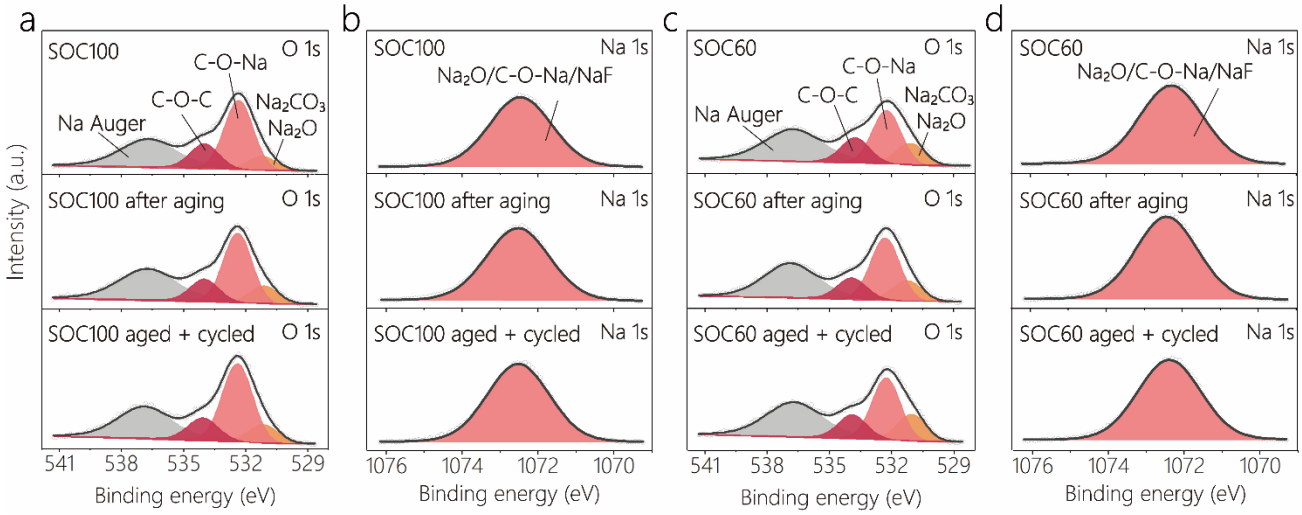

Fig. S15. XPS spectra of O 1s (a, c) and Na 1s (b, e) of graphite anodes. Na Auger peaks is located at 536.6 eV in O 1s, which is eliminated in the calculation of O content.

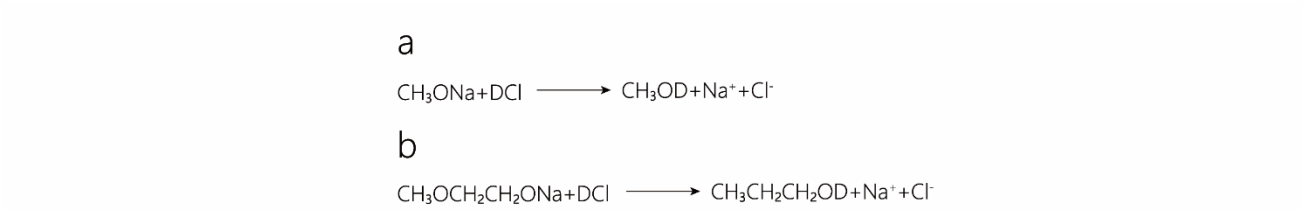

Fig. S16. Chemical reaction of diglyme-derived SEI components in the 0.1 M DCl D_2O solution.

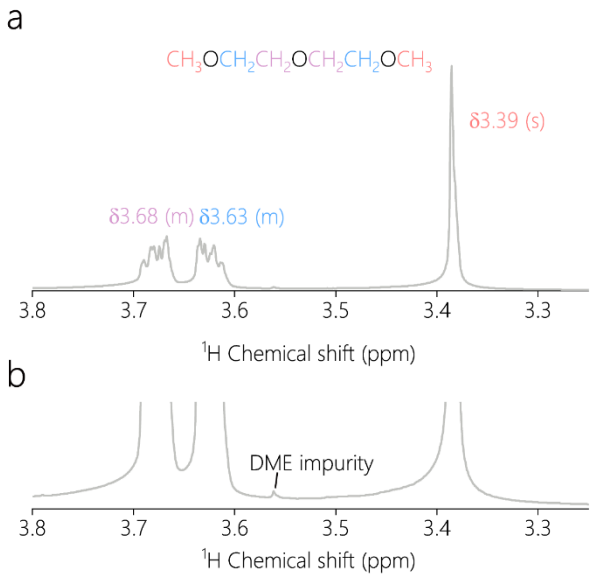

Fig. S17. ^{1}H NMR spectra of 1 M $NaPF_6$ diglyme electrolyte (a) and enlarged version for comparison (b).

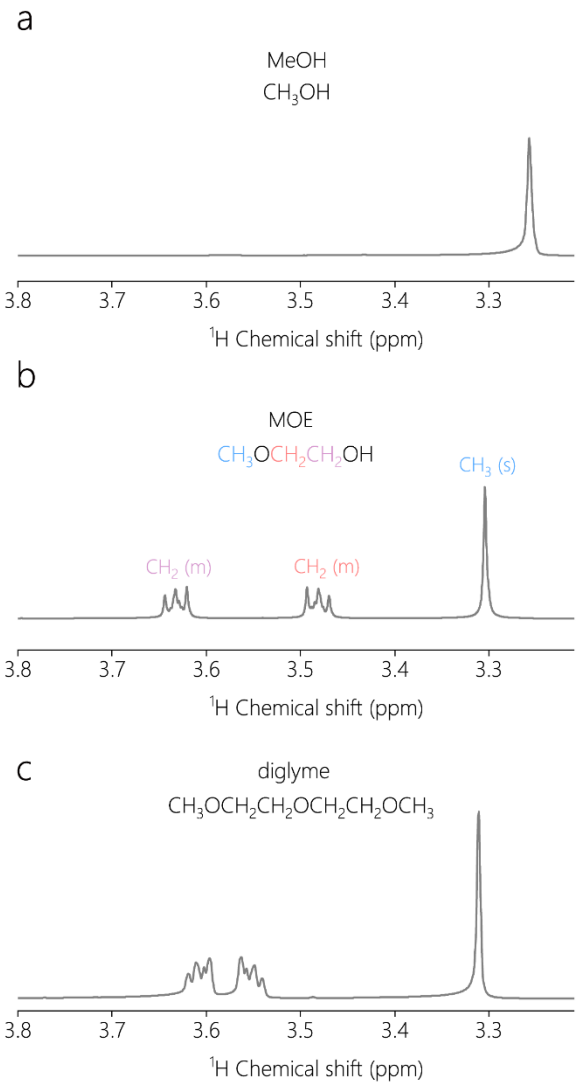

Fig. S18. (a–c) ^{1}H NMR spectra of methanol (a), 2-meyhoxyethanol (MOE) (b) and diglyme (c). The first CH_2 in $CH_3OCH_2CH_2OH$ shows low ppm than diglyme and the second CH_2 in $CH_3OCH_2CH_2OH$ is at high ppm than diglyme. The CH_3 of MOE and diglyme appear at the similar position.

References

1 J. Wang, H. Wang, R. Zhao, Y. Wei, F. Kang, D. Zhai, *Nano Lett.* **2022**, 22, 6359-6365.

2 T. H. Wan, M. Saccoccio, C. Chen, F. Ciucci, *Electrochimica Acta* **2015**, 184, 483-499

3 J. Chen, E. Quattrocchi, F. Ciucci, Y. Chen, *Chem* **2023**, 9, 2267-2281.

4 H. Kim, J. Hong, G. Yoon, H. Kim, K.-Y. Park, M.-S. Park, W.-S. Yoon, K. Kang, *Energy Environ. Sci.* **2015**, 8, 2963-2969.

5 C. B. Mustafa Goktas, Erik J. Berg, Petr Novák, Kilian Pollok, Falko Langenhorst, Maximilian v. Roeder, Olena Lenchuk, Doreen Mollenhauer, and Philipp Adelhelm, *Adv. Energy Mater.* **2018**, 8, 1702724.